

Direct oxygen measurements of Cr-rich spinel: Implications for spinel stoichiometry

MARCEL KAMPERMAN,^{1,*} LEONID V. DANYUSHEVSKY,¹ WAYNE R. TAYLOR,^{2,†} AND
WIESLAV JABLONSKI³

¹Department of Geology, University of Tasmania, GPO Box 252C, Hobart, Tasmania 7001, Australia

²Crystallography and Mineral Physics Unit, Department of Geological Sciences, University College, London, U.K.

³Central Science Laboratory, University of Tasmania, GPO Box 252C, Hobart, Tasmania 7001, Australia

ABSTRACT

The availability of a synthetic multilayer crystal and accurately calibrated oxide and silicate standards make it possible to use the electron microprobe for precise O analysis of spinel. A requirement of the O measurement routine described is the use of repetitive statistical analyses of the O standards and subsequent corrections and recalibration. A representative set of O analyses for each spinel population studied is essential to obtain reliable data, and the danger of using single datum is emphasized. Magnesiochromite spinel grains, having broad compositional similarities but different petrogenetic and cooling histories, were analyzed for O and their stoichiometry was assessed. Diamond-indicator spinel from the Aries kimberlite and Argyle lamproite is stoichiometric. Spinel inclusions in olivine phenocrysts from Ti-poor tholeiite from the Hunter Fraction Zone and Ca-rich boninite from the Tonga Trench show a range of nonstoichiometry. High $\text{Fe}^{2+}/\text{Fe}^{3+}$ values calculated assuming stoichiometry for such spinel are invalid. Spinel samples from metamorphosed volcanics from the Peak Hill–Glengarry Basin and the Heazlewood River Ultramafic Complex are also nonstoichiometric, having significant $\text{Fe}_{0.3}\text{O}_4$ – $\text{Cr}_{0.3}\text{O}_4$ components. Our results demonstrate that nonstoichiometry is a common feature of Cr-rich spinel. This has important implications for the use of Fe^{3+} and Fe^{2+} concentrations to estimate the oxidation state or temperature of formation.

INTRODUCTION

Experimental studies of spinel within the Fe–Ti–O ternary have demonstrated substantial nonstoichiometry, which is a function of temperature, composition, and f_{O_2} (e.g., Aragon and McCallister 1982). The stoichiometry of natural Cr–Al-bearing spinel has also been a matter of recent debate (e.g., Wood and Virgo 1989; Ballhaus et al. 1991; Carmichael 1991). One important parameter of spinel composition dependent on stoichiometry is the $\text{Fe}^{3+}/\text{Fe}^{2+}$ value. From electron microprobe analytical data, the $\text{Fe}^{3+}/\text{Fe}^{2+}$ value may be calculated by assuming that the spinel structure has a perfect stoichiometry with three cations per four O atoms. Stoichiometry calculations are based on the assumption of charge balance, with Fe as the only cation with a variable valency state (e.g., Finger 1972). It has been demonstrated that the $\text{Fe}^{3+}/\text{Fe}^{2+}$ value is a potential f_{O_2} indicator, and several experimentally calibrated olivine–orthopyroxene–spinel O_2 geobarometers have been developed on this basis (O'Neill and Wall 1987; Mattioli and Wood 1988; Ballhaus et al. 1991).

Ballhaus et al. (1990, 1991) and McGuire et al. (1989) demonstrated that for some samples of spinel, Fe^{3+} calculated from electron microprobe analyses assuming stoichiometry agrees well with Fe^{3+} independently measured by Mössbauer spectroscopy. On the other hand, Wood and Virgo (1989) and Carmichael (1991) showed that spinel from abyssal lherzolite assemblages is significantly nonstoichiometric according to Fe^{3+} analyses by Mössbauer spectroscopy. Because spinel often occurs as small grains and inclusions in other minerals, Mössbauer spectroscopy cannot be widely applied because it requires a relatively large sample size. To overcome this problem, we developed an O measurement technique, using an electron microprobe (e.g., Nash 1992), that allows an accurate assessment of stoichiometry and calculation of Fe^{3+} content in individual spinel grains.

In this paper we discuss results of O analyses of Cr-rich spinel having broad compositional similarities from both high- and low-pressure mantle-derived suites. Such spinels are widely used as petrogenetic indicators. Cr-rich xenocrystic spinel found in kimberlite and lamproite [magnesiochromite with $\text{Cr}' = 100\text{Cr}/(\text{Cr} + \text{Al})$ of 70–95, $\text{Mg}' = 100\text{Mg}/(\text{Mg} + \text{Fe}^{2+})$ of 50–80 and $\text{Fe}^{3+}/\Sigma\text{Fe} < 0.3$] is often used as diamond indicators (e.g., Haggerty 1979; Ramsay 1992; Kamperman et al. 1993). A typical feature of many diamond-indicator spinel compositions

* Present address: BHP Iron Ore Pty Ltd., P.O. Box 655, Newman, Western Australia 6753, Australia.

† Present address: Research School of Earth Sciences, Australian National University, Canberra, ACT 0200, Australia.

is that, when recalculated from metal-oxide analyses assuming stoichiometry, all Fe is present as Fe^{2+} and small amounts of Cr may also be present as Cr^{2+} (e.g., Haggerty 1979). Such compositional features are believed to be consistent with their formation in the upper mantle at the high-pressure reduced conditions of diamond stability (Haggerty 1986).

Cr-rich spinel from primitive subduction-related magmatic suites has $\text{Fe}^{2+}/\text{Fe}^{3+}$ values calculated according to stoichiometry that extend to very high values, particularly in some boninitic suites (e.g., Sigurdsson et al. 1993; Sobolev and Danyushevsky 1994). If valid, the observed range would imply reduced crystallization conditions for many subduction-related suites in contradiction of the generally accepted oxidized nature of magmas generated in subduction zones (e.g., Ballhaus et al. 1991).

We use our O measurement technique to demonstrate that nonstoichiometry is a common feature of Cr-rich spinel, and we argue that the possibility of spinel nonstoichiometry must be taken into account in petrologic applications.

ANALYTICAL METHOD

Design of analytical routine

The USNM 111989 gahnite from Brazil (Jarosewich et al. 1980) was used as a mineral standard for calibration of O. We chose this spinel standard because its mean atomic number ($Z_{\text{calc}} = 16.10$) is comparable to that of Cr-rich spinel (e.g., $Z_{\text{calc}} = 16.29$ for USNM 117075 chromite standard; Jarosewich et al. 1980). The gahnite standard was analyzed for O by fast neutron activation analysis (FNAA, McGuire et al. 1992), and O_{FNAA} of 35.20 wt% (1σ 0.57) compares well with O_{calc} (from electron microprobe metal-oxide analyses) of 34.92 wt%, suggesting that the spinel standard is stoichiometric (McGuire et al. 1992). The average value of 35.06 wt% is accepted here as the gahnite O content.

All analyses were performed on a Cameca SX-50 electron probe microanalyzer (EPMA) at the University of Tasmania in Hobart. A PC1 W/Si (2d = 6 nm) multilayer crystal in an inclined spectrometer was used for measurement of O. The remaining spectrometers were set with TAP and LiF analyzing crystals. A multipurpose analytical routine designed to analyze the O content of minerals was programmed to include Mg (TAP crystal, USNM 117075 chromite standard), Al (TAP crystal, USNM 111989 gahnite standard), Si (TAP crystal, USNM R17701 quartz standard), Ti (LiF crystal, Astimex MIMN 25–53 rutile standard), Cr (LiF crystal, USNM 117075 chromite standard), Mn (LiF crystal, Astimex MIMN 25–53 rhodonite standard), Fe (LiF crystal, USNM 96189 ilmenite standard), Ni (LiF crystal, Astimex MIMN 25–53 nickel silicide standard), V (LiF crystal, pure vanadium), and Zn (LiF crystal, USNM 111989 gahnite standard). Metal-oxide concentrations of spinel inclusions in olivines from modern subduction-related suites were analyzed using a separate analytical routine, which differed

in that Cr and Ti were analyzed on a PET crystal, and the results were combined with O contents analyzed using the first routine. For both routines, analyses were performed at 15 keV accelerating voltage, an electrical beam current of 20 nA, and a beam diameter varying from 1 to 10 μm at a 10000 \times magnification. O was analyzed at the beginning of each analysis; counting time was 40 s on the peak and 20 s on the background measured on both sides of the analytical peak. All other elements were analyzed at 10 s on the peak and 5 s on the background. For these counting times the calculated tolerance, which is the detection limit (at 2σ) divided by the weight percent concentration, for the major cations is <1% (relative), which is within the quoted total precision of 2% (relative) of the analytical system. Concentrations were calculated from relative peak intensities using the PAP matrix correction procedure (Pouchou and Pichoir 1991). On the gahnite standard containing 35.06 wt% O, the analytical conditions yielded a peak-to-background ratio for O of 93, comparable to that of Al (82) and better than Zn (62).

Probe mounts of mineral grain composites under investigation were made using cold-set epoxy. Care was taken to obtain a high-quality polish, using various grades of diamond-polishing paste. Sample probe mounts and the standard probe mount were coated at the same time with a thin film of ultra-high-purity carbon, ensuring uniformity of coating of standards and samples.

Analytical procedure

The O standards were recalibrated at the beginning of each analytical session. The gahnite O standard was checked at regular intervals (after every 5–10 analyses) during each analytical session, and crystal reverifications or recalibrations were made when the value of $\text{O}_{\text{analyzed}}$: $\text{O}_{\text{accepted}}$ was <0.98 or >1.02. Each analysis represents an average of two or three analytical points, always taken from the same area of the standard grain to avoid any possibility of incorporating standard nonhomogeneity. The unknown grains were analyzed over very small areas (generally ~ 10 μm apart) and did not involve core-to-rim analyses, thus avoiding the possibility of grain nonhomogeneity. Analytical values quoted for unknown grains also represent an average of two or three analytical points, and for O and the major cations these values demonstrate a precision better than 2% (relative).

O data corrections (in terms of O by weight percent) were made by adjusting the analytical results when a systematic shift (Figs. 1A and 1B) or consistent regular drift occurred (Fig. 1C) between two adjacent sets of standard analyses. To check the reliability of the corrected data obtained during intervals when the standard drift occurred, analyses of some grains were repeated after verification and compared with the corrected value. Table 1 illustrates the results of this procedure from analyses on the same spinel grain (an inclusion in olivine from a Tongan boninite) during an analytical session before and after verification. The results demonstrate a precision better than 2% (relative).

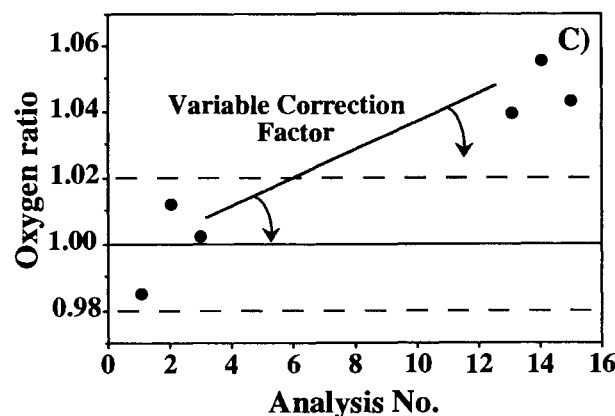
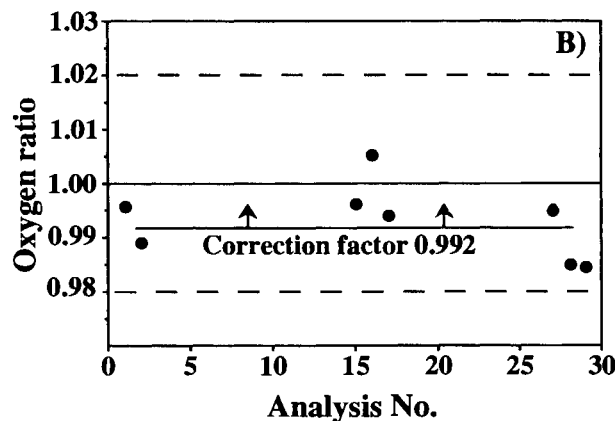
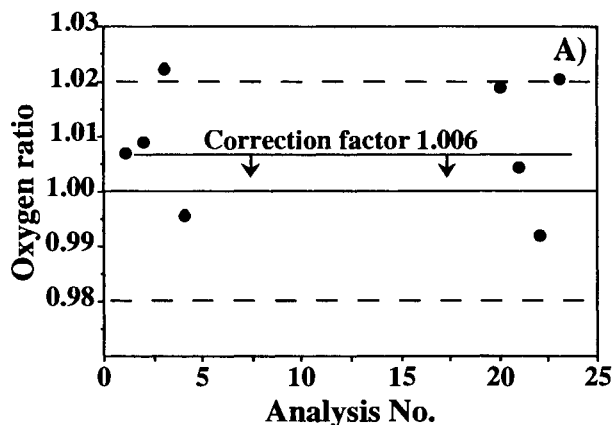


FIGURE 1. (A and B) Correction method used for adjusting O analytical results if a systematic standard shift occurred upward (A) or downward (B) during an analytical session. O data for a session were adjusted by an average correction factor calculated from the ratio (= O ratio) of the measured O content to the accepted O content of 35.06 wt% for the gahnite standard. (C) Correction method used for adjusting O analytical results if standard drift occurred during an analytical session. O data for a session were adjusted by a variable correction factor calculated from the O ratio. The O ratio between 0.98 and 1.02 indicates the range of acceptable measured O values from the gahnite standard. See text for recalibration and reverification procedure used if the ratio was <0.98 or >1.02 .

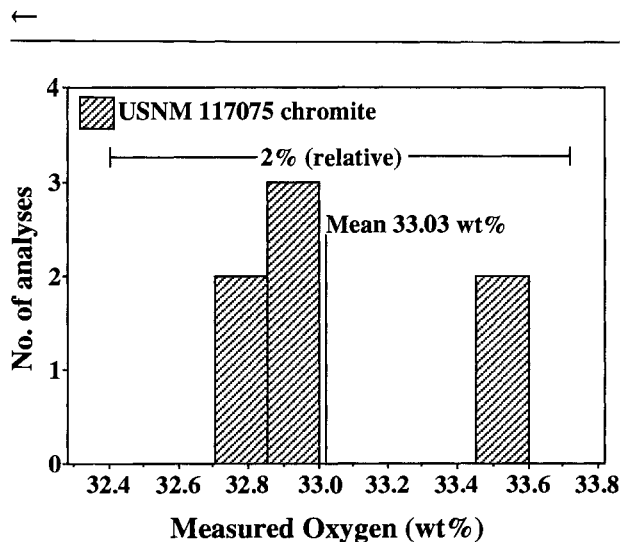


FIGURE 2. Frequency histogram of repetitive O analyses of the USNM 117075 chromite during an analytical session. The chromite has an average O content of 33.03 wt%. The error bar indicates 2% (relative) of the mean.

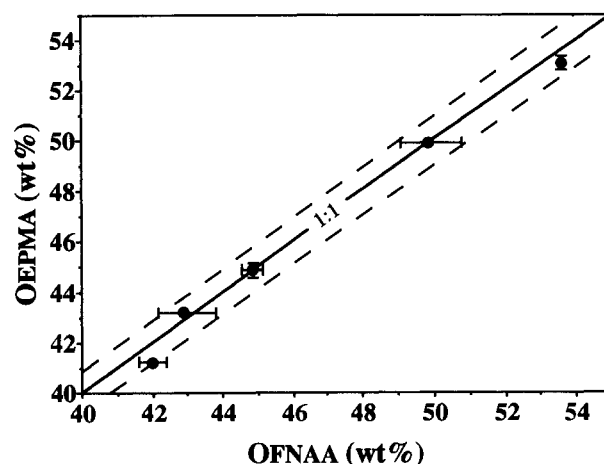


FIGURE 3. Comparison of O of secondary standards (see Table 2 for details) measured by electron microprobe vs. O measured using the fast neutron activation technique (McGuire et al. 1992). The dashed lines indicate 2% (relative) of the mean. Error bars (shown only if error is larger than the size of the symbol) represent standard deviations.

TABLE 1. Procedure for correcting O data following standard drift during an analytical session

No. Analyses Sample	1 1-3 Gahnite	2 11-12 5-28/OL10-SP	3 13-15 Gahnite	4 5-28/OL10-SP (corrected)	5 16-18 Gahnite (recalibrated)	6 19-20 5-28/OL10-SP (new)	7 21 Gahnite
O (wt%)	34.99(0.39)	33.02(0.08)	36.62(0.25)	31.61	34.98(0.27)	31.53(0.26)	34.96
O _{ratio}	0.9980		1.0445		0.9977		0.9971

Note: The O analyses were obtained in one continuous session. The row labeled "Analyses" indicates the order of samples analyzed during the session. Data shown are average values of corresponding points, with data in parentheses representing standard deviations. O_{ratio} values were obtained by O_{meas}/O_{accepted} for the gahnite standard of McGuire et al. (1992). See text for discussion.

The cation standards were checked at the beginning of each analytical session, and recalibrations were made when the value of $\text{cation}_{\text{analyzed}}:\text{cation}_{\text{standard}}$ was <0.98 or >1.02 . The USNM 117075 chromite standard was checked at the beginning and the end of each analytical session, and for the duration of a given analytical session cation drift did not exceed 1% (relative). Only analyses with totals (which equal the sum of cations plus O_{meas}) between 98.5 and 101.0 wt% were accepted.

Accuracy of O measurements

Repetitive analyses of the same grain performed during one analytical session (Fig. 2) show deviations $<2\%$ (relative). To enable comparison of the data analyzed during different analytical sessions, we analyzed several grains during different sessions. For example, data for sample 5-28/OL5-SPA are 31.02 and 31.16 wt% O. An average of 31.09 wt% was accepted as the O content. Data for sample 5-28/OL8-SPB are 32.62 and 32.82 wt% O. An average of 32.72 was accepted as the O content. Finally, analyses of secondary standards with known O content analyzed by FNA (Table 2 and Fig. 3) all imply that there is no systematic error in the analytical routine introduced by PAP matrix corrections, and that the precision is 2% (relative).

RESULTS

The following parameters are used in this paper: (1) Σ_{cations} is the sum of cations calculated on the basis of 4 O atoms, assuming all Fe is present as Fe²⁺ and all Cr is present as Cr³⁺. (2) O_{calc} is weight percent O calculated from metal-oxide compositions assuming stoichiometry. If our analyses indicated a possible presence of Cr²⁺ (i.e., Σ_{cations} was <3), we did not incorporate this effect into our calculations because our analyses did not result in a Σ_{cations} deficiency beyond the accuracy of the electron microprobe analyses. (3) $\Delta\text{O} = \text{O}_{\text{meas}} - \text{O}_{\text{calc}}$ is the deviation from stoichiometry. (4) O_{max} is the calculated O content assuming that all Fe is present as Fe³⁺, all Cr as Cr³⁺, all Mn as Mn²⁺; O_{min} is the calculated O content assuming all Fe is present as Fe²⁺.

If Cr²⁺ is not present, O_{meas} is expected to be between O_{max} and O_{min}; if O_{meas} is less than O_{min}, this may indicate that Cr²⁺ is present. Assuming that no other elements but Fe and Cr can be present in variable oxidation states (+2 or +3), O_{meas} is not expected to be larger than O_{max}.

Because O has a low atomic number in comparison with Fe, the established 2% (relative) accuracy of our O analyses corresponds to very large differences in calculated Fe²⁺ and Fe³⁺. For example, 2% (relative) O for a typical Cr-rich spinel is ~ 0.65 wt%, which corresponds

TABLE 2. O analyses of O standards (values in wt%)

Sample USNM no.	Gahnite 111989	Quartz 122838	Kaersutite 131928	Albite 131705	Olivine 131929	Almandine 112140
O _{EPMA}	34.99(0.39)	53.05(0.31)	43.22(0.14)	49.95(0.16)	44.93(0.27)	41.25(0.08)
O _{FNA}	35.20(0.57)	53.55(0.07)	42.87(0.83)	49.83(0.87)	44.8(0.30)	41.94(0.39)
O _{calc}	34.92	53.25	43.05	48.65	43.98	41.87
Si		46.74	18.51	31.82	19.58	17.95
Al	29.28		7.82	10.47		11.91
Fe ²⁺	1.53		0.56		6.86	19.78
Fe ³⁺			8.63	0.06		0.83
Mg			7.49		29.76	5.03
Mn	0.29		0.09		0.10	1.69
Ti			3.11			0.03
Cr						0.03
Ca			7.45	0.17	0.02	1.24
Na			2.09	8.49	0.01	0.09
K			1.19	0.22		
Ni					0.34	
Zn	34.14					
H			0.01			

Note: O_{EPMA} values determined in this work using an electron microprobe analyzer. O_{FNA} values determined by McGuire et al. (1992) using fast neutron activation analysis. O_{calc} values calculated by McGuire et al. (1992) assuming perfect charge balance and using measured H contents and Fe³⁺/Σ Fe values where applicable. Values in parentheses represent standard deviations. Major elements determined by Jarosewich et al. (1980).

TABLE 3. Representative analyses of diamond-indicator spinel (values in wt%)

No.	1	2	3	4	5	6
Locality	Argyle	Aries	Aries	Aries	Aries	Aries
Grain no.		13	8	12	11	5
Type	Lmp	Kmb	Kmb	Kmb	Kmb	Kmb
Si	0.04 (± 0.01)	0.02	0.02	0.05	0.02	0.02
Ti	0.02 (± 0.00)	0.03	0.00	0.14	0.23	0.02
Al	2.15 (± 0.47)	5.81	4.89	3.41	5.99	6.17
Cr	47.01 (± 0.87)	42.20	43.74	45.71	40.65	41.75
V	0.09 (± 0.01)	0.12	0.10	0.16	0.12	0.12
Fe	10.61 (± 0.21)	10.63	10.94	9.77	11.52	10.42
Mg	7.37 (± 0.04)	7.63	7.25	7.25	7.29	7.78
Mn	0.22 (± 0.04)	0.22	0.20	0.22	0.26	0.22
Ni	0.05 (± 0.02)	0.06	0.08	0.04	0.06	0.07
Zn	0.05 (± 0.04)	0.10	0.11	0.09	0.07	0.11
O	31.83 (± 0.35)	32.59	32.53	31.94	32.77	33.44
Total	99.43 (± 0.56)	99.40	99.86	98.77	98.98	100.12
O _{calc}	31.70 (± 0.12)	32.91	32.62	32.02	32.53	33.06
ΔO	0.13 (± 0.21)	-0.32	-0.09	-0.08	0.24	0.36
Σ_{cations}	3.001	2.997	2.994	2.983	3.000	2.997
O _{min}	31.69	32.91	32.62	32.02	32.53	33.06
O _{max}	33.21	34.44	34.19	33.42	34.18	34.55
FeO (corr.)	13.65	13.68	14.08	12.57	14.82	13.41
Fe ₂ O ₃ (corr.)	0	0	0	0	0	0

Note: Kmb = kimberlite, Lmp = lamproite. Analysis no. 1 is an average of five analyses of individual grains; numbers in parentheses give the range of individual analyses. See the beginning of the Results section for the definition of parameters of spinel compositions used in this table. FeO (corr.) = wt% of FeO present in spinel as calculated from O measurements. Fe₂O₃ (corr.) = wt% of Fe₂O₃ present in spinel as calculated from O measurements.

to 2.9 wt% FeO or 2.16 wt% Fe₂O₃. This demonstrates the danger of using individual O analyses for estimations of real spinel Fe²⁺/Fe³⁺ values and for assessing the existence of nonstoichiometry. Because of this, we employed a statistical approach to the O data. We considered average ΔO when the difference between individual ΔO values did not exceed 2% (relative) of O_{meas} and either analyzed spinels showed similar cation contents (inside the microprobe accuracy) or no correlation existed between ΔO and cation concentrations. Where a good correlation existed between ΔO and cation concentrations [standard deviations < 2% (relative) of O concentrations], a line of best fit illustrating ΔO as a function of cation

composition was selected to represent a sample population, rather than a single average composition.

Diamond-indicator spinel

We analyzed five spinel grains from the Middle Proterozoic diamond-bearing Argyle olivine lamproite diatreme in the East Kimberley region of Western Australia (Jaques et al. 1986). These grains occur as ~1 mm xenocrysts in the lamproite matrix. They are characterized by a very constant composition, including O, and the average of the analyses is shown in Table 3 (no. 1). According to our cation analyses, these spinel grains are stoichiometric with all Fe present as Fe²⁺. O contents (in

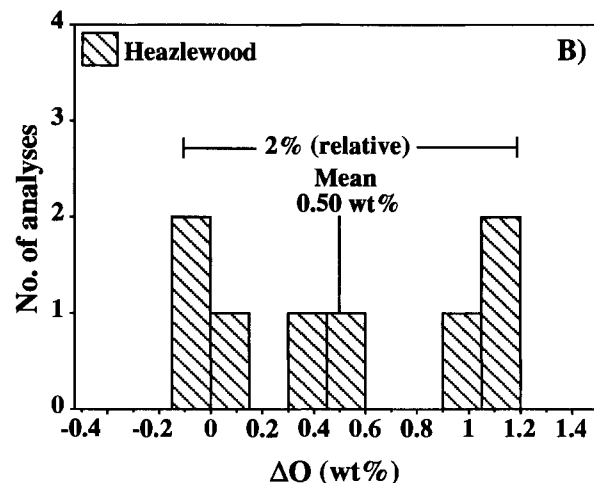
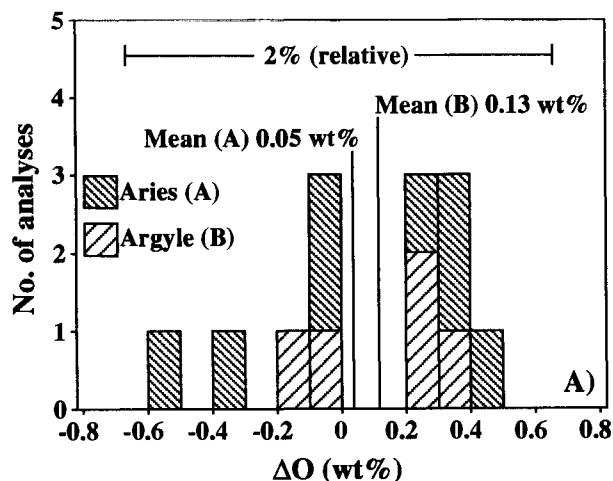


FIGURE 4. (A) Frequency histogram of ΔO for spinel from the Aries kimberlite and Argyle lamproite. The error bar indicates 2% (relative) of the mean. (B) Frequency histogram of ΔO

for spinel from the metamorphosed Heazlewood River Ultramafic Complex. The error bar indicates 2% (relative) of the mean.

TABLE 4. Representative analyses of spinel inclusions in olivine phenocrysts from primitive subduction-related magmas (values in wt%)

No.	1	2	3	4	5	6	7	8	9	10
Grain no.	115-4/H1 OL80-SP	115-4/H1 OL15E-SP	115-4/H1 OL88-SP	115-4/H1 OL77A-SP	115-4/H1 OL19-SPA	5-24/ OL3-SP	5-24/ OL3A-SPC	5-24/ OL27-SP	5-24/ OL4-SPA	5-24/ OL4-SPB
Type	Thol	Thol	Thol	Thol	Thol	Bon	Bon	Bon	Bon	Bon
Si	0.04	0.05	0.05	0.04	0.03	0.03	0.03	0.03	0.04	0.05
Ti	0.13	0.07	0.05	0.06	0.10	0.07	0.06	0.02	0.05	0.04
Al	6.57	5.20	5.21	5.22	5.57	3.29	3.45	3.47	3.28	3.23
Cr	34.59	38.29	36.78	37.07	36.89	41.97	41.24	40.94	44.21	43.03
Fe	18.14	15.97	17.26	16.86	16.57	15.44	15.54	16.01	10.72	11.13
Mg	6.98	7.35	6.80	6.98	7.04	7.07	7.07	6.88	8.43	8.25
Mn	0.22	0.28	0.21	0.22	0.20	0.20	0.23	0.24	0.16	0.17
Ni	0.07	0.09	0.05	0.06	0.08	0.06	0.06	0.06	0.04	0.09
Zn	0.09	0.03	0.06	0.02	0.05	0.06	0.03	0.08	0.09	0.04
O	32.67	32.62	32.64	32.85	33.14	32.06	32.08	32.20	33.15	32.71
Total	99.49	99.96	99.10	99.37	99.68	100.26	99.79	99.93	100.17	98.73
O _{calc}	32.71	32.64	31.99	32.11	32.29	32.14	32.00	31.91	32.42	31.90
ΔO	-0.04	-0.02	0.65	0.74	0.85	-0.08	0.08	0.29	0.73	0.81
Σ _{cations}	3.079	3.062	3.071	3.070	3.065	3.053	3.056	3.059	3.027	3.033
O _{min}	31.88	31.98	31.26	31.99	31.61	31.60	31.42	31.30	32.15	31.56
O _{max}	34.48	34.27	33.73	33.81	33.98	33.81	33.65	33.59	33.68	33.15
FeO (st)	15.90	14.64	15.64	15.23	15.25	14.95	14.78	15.13	11.30	11.22
Fe ₂ O ₃ (st)	8.26	6.56	7.30	7.17	6.74	5.46	5.79	6.08	2.77	3.44
Fe ²⁺ /Fe ³⁺ (st)	2.138	2.479	2.382	2.359	2.513	3.041	2.835	2.765	4.532	3.622
FeO (corr.)	16.25	14.82	9.77	8.60	7.55	15.70	14.08	12.48	4.78	3.97
Fe ₂ O ₃ (corr.)	7.88	6.37	13.83	14.54	15.30	4.64	6.58	9.02	10.02	11.50
Fe ²⁺ /Fe ³⁺ (corr.)	2.292	2.585	0.785	0.659	0.549	3.763	2.377	1.537	0.530	0.384
Fo	88.00	89.44	88.21	88.55	89.04	88.70	88.70	88.62	93.26	93.26

Note: Thol = tholeiite, Bon = boninite. Analyses 1–5 = spinel inclusions from Ti-poor tholeiite from the Hunter Fracture Zone. Analyses 6–10 = spinel inclusions from Ca-rich boninite from the northern Tonga Trench. See the beginning of the Results section for the definition of parameters of spinel compositions used in this table. Abbreviation st = values calculated assuming stoichiometry from cation analyses; corr. = values calculated on the basis of O data. During cation analyses of these spinels, V was not included in the analytical label. V₂O₅ of 0.15 wt% assumed in all recalculations. This assumption is based on the results obtained by Sobolev and Danyushevsky (1994) and Danyushevsky (unpublished data), who analyzed many spinel inclusions from the same samples. Results indicated a value for V₂O₅ of 0.15 ± 0.07 wt%, with no correlation to other element concentrations.

terms of ΔO) of the individual spinels are shown in Figure 4A. The variations between individual analyses are well inside the precision, and an average of 31.83 wt% was accepted as the O content of these spinels. Thus, our results lead to ΔO of +0.13 wt%. Although this may indicate a low degree of nonstoichiometry with some Fe present as Fe³⁺, we believe that the existing data are insufficient for such a conclusion and rather show a good agreement between cation and O data, which indicate that Argyle spinel is stoichiometric with all Fe present as Fe²⁺.

We also conclude that spinel from the Lower Proterozoic diamond-bearing Aries kimberlite diatreme in the Kimberley region, Western Australia (Edwards et al. 1992) is stoichiometric on the basis of analyses of eight grains from a spinel concentrate. Like the Argyle spinel, these spinel grains occur as ~1 mm xenocrysts in the matrix. Despite the fact that they are characterized by some significant variations in cation contents (Table 3, nos. 2–6), the cation data indicate that, within error, all Fe is present as Fe²⁺, and the average spinel has ΔO of +0.05 wt% (Fig. 4A).

Spinel inclusions in olivine from primitive subduction-related magmas

Cr-rich spinel is a common liquidus mineral in primitive subduction-related suites. Usually it is found as inclusions (up to 50 μm in diameter but more often 15–20 μm in diameter) in olivine phenocrysts. Two suites de-

scribed here, Ti-poor tholeiite from the Hunter Fracture Zone, North Fiji Basin (Sigurdsson et al. 1993) (Table 4, nos. 1–5), and Tongan Ca-rich boninite (Sobolev and Danyushevsky 1994) (Table 4, nos. 6–10) are characterized by a large range of olivine compositions and subsequent variations in the compositions of spinel inclusions (Table 4, Fig. 5). Unlike the diamond-indicator spinel, all analyzed spinel grains have Σ_{cations} > 3, implying the presence of Fe³⁺ if this spinel is to be stoichiometric. Both suites demonstrate a positive correlation between Cr' and Fe²⁺/Fe³⁺ values calculated assuming stoichiometry (Fig. 5A). Spinel from the Hunter Fracture Zone shows a range of Fe²⁺/Fe³⁺ values from 1.9 to 2.5, and spinel from Tongan boninite shows a range from 2.1 to 5.2.

Unlike the diamond-indicator spinel, O data for spinel inclusions in olivine phenocrysts from subduction-related suites show wide deviations from stoichiometry (–0.75 < ΔO < +1.9), which cannot be accounted for by the precision of the technique. Also, unlike the diamond-indicator spinel, these spinel grains show a good correlation between nonstoichiometry and spinel composition (Figs. 5B and 5C). Spinel Fe²⁺/Fe³⁺ values calculated according to stoichiometry correlate with ΔO. This leads to corrected (i.e., actual) Fe²⁺/Fe³⁺ values (Table 4) that are significantly lower for spinel with high Fe²⁺/Fe³⁺.

Results obtained are of particular importance for estimating MgO contents (and consequently liquidus temperatures) of primitive subduction-related melts that were in equilibrium with Cr-rich spinels and their olivine hosts.

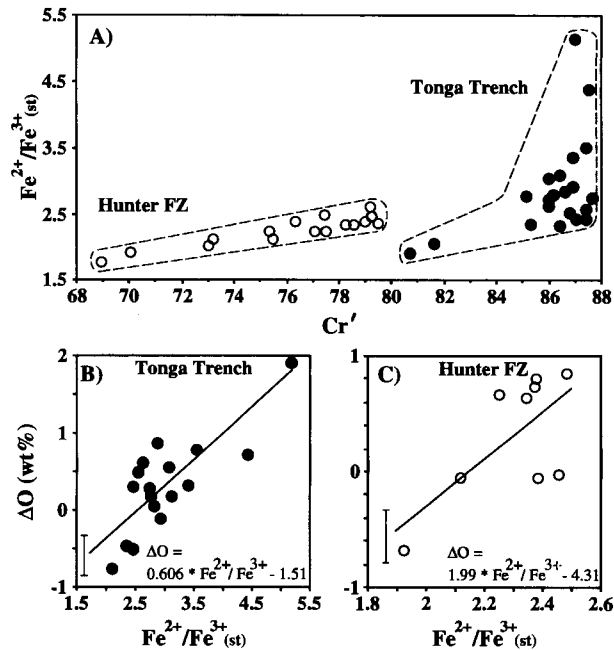


FIGURE 5. (A) $\text{Fe}^{2+}/\text{Fe}^{3+}$ vs. Cr' for spinel inclusions in olivine from Ti-poor tholeiite from the Hunter Fraction Zone and Tongan Ca-rich boninite. $\text{Fe}^{2+}/\text{Fe}^{3+}$ is calculated assuming spinel stoichiometry. (B and C) Plot of ΔO vs. $\text{Fe}^{2+}/\text{Fe}^{3+}$ for spinel inclusions from the Tongan boninite and the Hunter Fraction Zone tholeiite, respectively. The equations for ΔO as a function of $\text{Fe}^{2+}/\text{Fe}^{3+}$ represent lines of best fit. Calculated regression coefficients for the lines of best fit in B and C are 0.78 and 0.68, respectively. The error bars indicate 2% (relative) of the mean.

Indeed, the Mg' of such melts can be inferred using well-known parameters of olivine-melt equilibria (e.g., Ford et al. 1983). Thus, MgO contents are a function of Fe^{2+} concentrations, which, in turn, are dependent on f_{O_2} (e.g., Kress and Carmichael 1988). The high $\text{Fe}^{2+}/\text{Fe}^{3+}$ values calculated in the most primitive Cr-rich spinel according to stoichiometry would lead to erroneously low f_{O_2} values when calculated using a spinel O geosensor. This, in turn, would lead to erroneously high Fe^{2+} and, as a result, high MgO in primitive subduction-related melts.

Our results indicate that f_{O_2} cannot be correctly estimated assuming stoichiometry and using the cation compositions of Cr-rich spinel from primitive subduction-related magmas. Correct estimations of f_{O_2} for these suites remain a problem, as even known accurate cation compositions of nonstoichiometric spinel are not sufficient for f_{O_2} calculation, because the effect of cation deficiency (or excess) on the activity of elements in Cr-rich spinel is unknown.

Spinel from metamorphosed volcanic rocks

We also analyzed two populations of Cr-rich spinel from old volcanic complexes of boninitic affinity, the weakly metamorphosed Upper-Middle Cambrian Heazlewood River Ultramafic Complex, Western Tasmania (Peck 1990), and the Middle Proterozoic graywackes and volcanic rocks from the greenschist facies Glengarry Group in the Peak Hill area, central Western Australia (Hynes and Gee 1986). Although a magmatic origin has been suggested for both spinel populations, these spinels, un-

TABLE 5. Representative analyses of spinel from metamorphosed volcanic rocks (values in wt%)

No.	1	2	3	4	5	6	7	8	9
Locality	Peak Hill	Peak Hill	Peak Hill	Peak Hill	Peak Hill	Peak Hill	Peak Hill	Peak Hill	Heazlewood
Grain no.	507	405	202	304	204	806	708	203	
Si	0.04	0.01	0.03	0.02	0.03	0.03	0.04	0.03	0.03 (± 0.01)
Ti	0.01	0.09	0.07	0.01	0.02	0.01	0.05	0.02	0.03 (± 0.00)
Al	1.46	2.76	1.69	1.67	1.54	1.46	1.79	1.85	3.20 (± 0.26)
Cr	48.31	42.00	47.73	47.40	46.76	47.39	44.72	45.89	42.56 (± 0.67)
V	0.01	0.01	0.01	0.01	0.01	0.01	0.01	0.01	0.04 (± 0.00)
Fe	9.39	19.20	8.16	9.87	11.49	10.67	14.91	12.29	17.28 (± 1.11)
Mg	7.08	2.05	7.52	6.50	5.66	5.52	3.46	5.20	5.26 (± 0.23)
Mn	0.53	1.41	0.90	0.99	0.81	1.04	0.83	0.60	0.24 (± 0.05)
Ni	0.12	0.01	0.10	0.06	0.05	0.10	0.05	0.00	0.04 (± 0.04)
Zn	0.06	0.56	0.43	0.27	0.36	0.77	0.95	1.37	0.07 (± 0.03)
O	33.04	31.33	33.37	33.06	32.76	32.88	32.07	33.33	31.88 (± 0.62)
Total	100.04	99.42	99.99	99.84	99.48	99.87	98.87	100.57	100.61 (± 0.68)
O_{calc}	31.25	29.36	31.34	30.91	30.40	30.47	29.39	30.37	31.38 (± 0.28)
ΔO	1.79	1.97	2.03	2.15	2.36	2.41	2.68	2.96	0.50 (± 0.65)
Σ_{cations}	2.988	3.002	2.992	2.989	2.989	2.982	2.985	2.994	3.030
O_{min}	31.25	29.36	31.34	30.91	30.40	30.47	29.39	30.37	31.06
O_{max}	32.59	32.11	32.50	32.33	32.04	32.00	31.53	32.13	33.53
FeO (st)	12.08	24.57	10.50	12.69	14.78	13.73	19.19	15.81	19.34
Fe_2O_3 (st)	—	—	—	—	—	—	—	—	3.21
$\text{Fe}^{2+}/\text{Fe}^{3+}$ (st)	—	—	—	—	—	—	—	—	6.703
FeO (corr.)	—	7.00	—	—	—	—	—	—	14.89
Fe_2O_3 (corr.)	13.43	19.67	11.66	14.11	16.42	15.26	21.32	17.57	8.16
$\text{Fe}^{2+}/\text{Fe}^{3+}$ (corr.)	—	0.395	—	—	—	—	—	—	2.029
% maghemite	52.4	56.2	57.2	61.7	68.3	71.2	79.6	81.8	—

Note: Analysis 9 is an average of eight analyses of individual grains; numbers in parentheses show the range of individual analyses. See the beginning of the Results section for the definition of parameters of spinel compositions used in this table. Abbreviation st = values calculated assuming stoichiometry from cation analyses; corr. = values calculated on the basis of O data; % maghemite = % of $\square_{1/3}\text{Me}_2\text{O}_4$ in spinel structure calculated on the basis of O data.

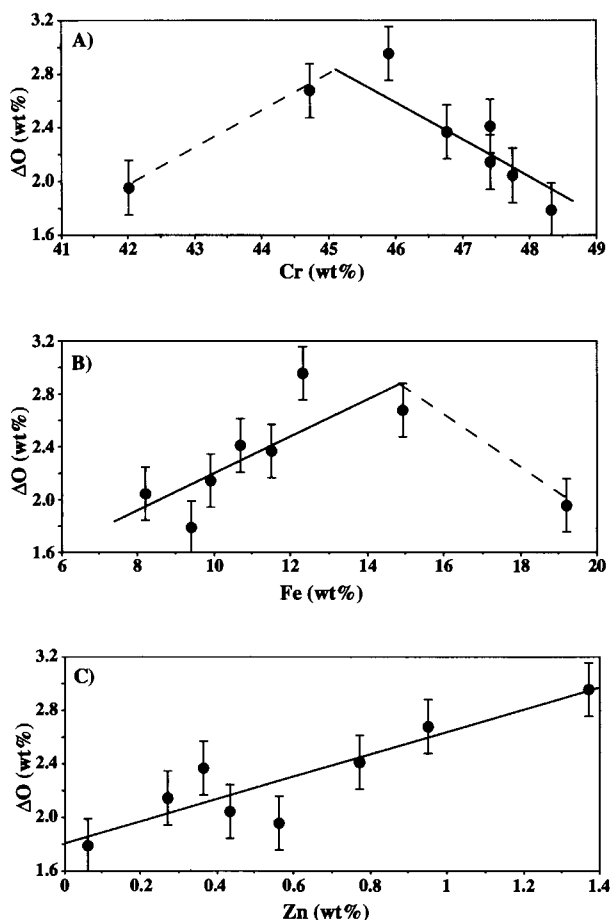


FIGURE 6. Plot of (A) ΔO vs. Cr, (B) ΔO vs. Fe, and (C) ΔO vs. Zn for spinel grains from the Glengarry Group in the Peak Hill area. The error bars indicate 2% (relative) of the mean.

like spinels described in the previous sections, have undergone metamorphic reequilibration.

We analyzed eight spinel grains from a spinel concentrate from the Peak Hill area. The grains are characterized by very high Cr_2O_3 contents (61–71 wt%), variably high Mn and Zn, and generally low Fe contents (Table 5) in comparison with the previously discussed spinel samples. According to cation analyses, they are stoichiometric with all Fe present as Fe^{2+} . Unlike diamond-indicator and boninitic spinel, these spinel grains have very high ΔO (+1.8 to +3 wt%), and a good correlation exists between ΔO and Zn, Fe, and Cr content (Fig. 6). With the exception of one spinel grain (Table 5, no. 2), the O_{meas} is significantly higher than O_{max} , which requires that all Mn is present as Mn^{3+} and that some Cr is present as Cr^{4+} to achieve electric neutrality. Although the presence of Cr^{4+} implies a very high oxidation state, minor amounts of Cr^{4+} have been reported in other minerals (e.g., rutile, Ishida et al. 1990). The relationships between O and cations indicate that these spinel grains deviate greatly from spinel stoichiometry and have compositions that lie between the Me_3O_4 and $\square_{1/3}\text{Fe}_8\text{O}_4$ – $\square_{1/3}\text{Cr}_8\text{O}_4$ (maghemite-

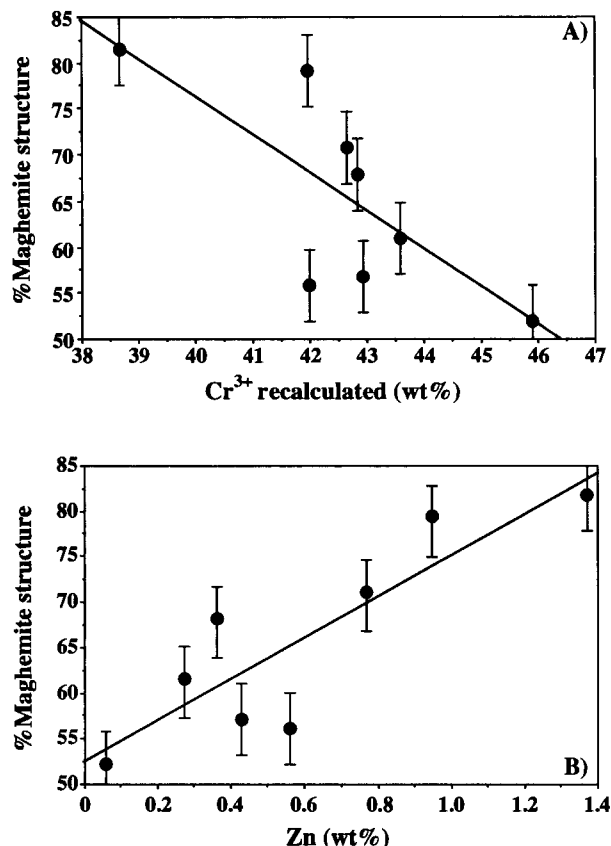


FIGURE 7. (A) Percent maghemite vs. $\text{Cr}^{3+}_{\text{recalc}}$ and (B) percent maghemite vs. Zn for spinel grains from the Glengarry Group in the Peak Hill area. Percent maghemite represents the amount of $\square_{1/3}\text{Me}_8\text{O}_4$ end-member and is calculated from the O data. $\text{Cr}^{3+}_{\text{recalc}}$ is calculated from the O data assuming all Fe is Fe^{3+} , all Mn is Mn^{3+} , and some Cr is Cr^{4+} to achieve electric neutrality. The error bars indicate 2% (relative) of the mean.

Cr equivalent of maghemite) end-members. To estimate the degree of nonstoichiometry of each analysis, we calculated the percent of $\square_{1/3}\text{Me}_8\text{O}_4$, which varies between 50 and 80% (Fig. 7).

Spinel from the Heazlewood Complex probably occurred originally as inclusions in mafic silicate phenocrysts. Eight analyzed grains have very similar cation compositions, and an average of the analyses is shown in Table 5 (no. 9). O data show variations inside 2% (relative) of O_{meas} , with a mean of $\Delta O = +0.5$ wt% (Fig. 4B), and because no correlation was observed between cation compositions and ΔO variations, an average of 31.88 wt% O was accepted as the O content of this spinel.

Our O data indicate that Heazlewood spinel is significantly nonstoichiometric, having an excess of 4.95 wt% $\square_{1/3}\text{Fe}_8\text{O}_4$ in comparison with stoichiometry.

CONCLUSIONS

Our results indicate that spinel nonstoichiometry may be a common occurrence in Cr-rich spinels. This has serious consequences when using Fe^{3+} in spinels to calcu-

late the f_{O_2} from heterogeneous mineral redox equilibria, or Fe^{2+} to calculate the temperature of formation from mineral exchange reactions.

ACKNOWLEDGMENTS

We thank Western Mining Corporation and the Department of Geology at the University of Western Australia for providing spinel concentrates from the Peak Hill–Glenarry Basin and the Aries kimberlite. We gratefully acknowledge support, encouragement, and constructive criticism from David Green, Tony Crawford, and members of the Petrology Discussion Group at the University of Tasmania. M.K. is supported by an Australian Postgraduate Research Award (Industry). We also thank associate editor W.P. Nash (University of Utah) and four reviewers for constructive reviews of the manuscript.

REFERENCES CITED

- Aragon, R., and McCallister, R.H. (1982) Phase and point defect equilibria in the titanomagnetite solid solution. *Physics and Chemistry of Minerals*, 8, 112–120.
- Ballhaus, C., Berry, R.F., and Green, D.H. (1990) Oxygen fugacity controls in the Earth's upper mantle. *Nature*, 348, 437–440.
- (1991) High pressure experimental calibration of the olivine-orthopyroxene-spinel oxygen barometer: Implications for the oxidation state of the upper mantle. *Contributions to Mineralogy and Petrology*, 107, 27–40.
- Carmichael, I.S.E. (1991) The redox states of basic and silicic magmas: A reflection of their source regions? *Contributions to Mineralogy and Petrology*, 106, 129–141.
- Edwards, D., Rock, N.M.S., Taylor, W.R., Griffin, B.J., and Ramsay, R.R. (1992) Mineralogy and petrology of the Aries diamondiferous kimberlite pipe, Central Kimberley Block, Western Australia. *Journal of Petrology*, 33, 1157–1191.
- Finger, L.W. (1972) The uncertainty of the calculated ferric iron content of a microprobe analysis. *Carnegie Institution of Washington Year Book*, 71, 600–603.
- Ford, C.E., Russel, D.G., Groven, J.A., and Fisk, M.R. (1983) Distribution coefficients of Mg^{2+} , Fe^{2+} , Ca^{2+} and Mn^{2+} between olivine and melt. *Journal of Petrology*, 24, 256–265.
- Haggerty, S.E. (1979) Spinel in high pressure regimes. In F.R. Boyd and H.O.A. Meyer, Eds., *The mantle sample: Inclusions in kimberlites and other volcanics*. Proceedings of the 2nd International Kimberlite Conference, volume 2, 183–196.
- (1986) Diamond genesis in a multiply-constrained model. *Nature*, 320, 34–39.
- Hynes, A., and Gee, R.D. (1986) Geologic setting and petrochemistry of the Naracoota Volcanics, Capricorn Orogen, Western Australia. *Precambrian Research*, 31, 107–132.
- Ishida, S., Hayashi, M., Fujimura, Y., and Fujiyoshi, K. (1990) Spectroscopic study of the chemical state and coloration of chromium in rutile. *Journal of the American Ceramic Society*, 73, 3351–3355.
- Jaques, A.L., Lewis, J.D., and Smith, C.B. (1986) The kimberlites and lamproites of Western Australia. Geological Survey of Western Australia, Bulletin 132, p. 268.
- Jarosewich, E., Nelen, J.A., and Norberg, J.A. (1980) Reference samples for electron microprobe analysis. *Geostandards Newsletter*, 4, 43–47.
- Kamperman, M., Taylor, W.R., Hamilton, R., and Jablonski, W. (1993) Major and trace element discrimination of magnesiochromites from boninitic and diamond-related sources. In 1993 General Assembly of the International Association of Volcanology and Chemistry of the Earth's Interior (IAVCEI) Abstracts, 55.
- Kress, V.C., and Carmichael, I.S.E. (1988) Stoichiometry of the iron oxidation reaction in silicate melts. *American Mineralogist*, 73, 1267–1274.
- Mattioli, G.S., and Wood, B.J. (1988) Magnetite activity across the $MgAl_2O_4$ - Fe_3O_4 spinel join, with application to thermobarometric estimates of upper mantle oxygen fugacity. *Contributions to Mineralogy and Petrology*, 98, 148–162.
- McGuire, A.V., Dyar, M.D., and Ward, K.A. (1989) Neglected Fe^{3+}/Fe^{2+} ratios: A study of Fe^{3+} content of megacrysts from alkali basalts. *Geology*, 17, 687–690.
- McGuire, A.V., Francis, C.A., and Dyar, M.D. (1992) Mineral standards for electron microprobe analysis of oxygen. *American Mineralogist*, 77, 1087–1091.
- Nash, W.P. (1992) Analysis of oxygen with the electron microprobe: Applications to hydrated glass and minerals. *American Mineralogist*, 77, 453–456.
- O'Neill, H.St.C., and Wall, V.J. (1987) The olivine-orthopyroxene-spinel oxygen geobarometer, the nickel precipitation curve, and the oxygen fugacity of the Earth's upper mantle. *Journal of Petrology*, 28, 1169–1191.
- Pouchou, J.L., and Pichoir, F. (1991) Quantitative analysis of homogeneous or stratified microvolumes applying the model "PAP." In K.F.J. Heinrich and D.E. Newbury, Eds., *Electron probe quantitation*, p. 31–75. Plenum, New York.
- Peck, D.C. (1990) The platinum-group element geochemistry and petrogenesis of the Heazlewood River Mafic/Ultramafic Complex, Tasmania. Ph.D. thesis, University of Melbourne, Australia.
- Ramsay, R.R. (1992) The geochemistry of diamond indicator minerals. Ph.D. thesis, University of Western Australia, Perth.
- Sigurdsson, I.A., Kamenetsky, V.S., Crawford, A.J., Eggins, S.M., and Zlobin, S.K. (1993) Primitive island arc and oceanic lavas from the Hunter Ridge–Hunter Fracture Zone: Evidence from glass, olivine and spinel compositions. *Mineralogy and Petrology*, 47, 149–169.
- Sobolev, A.V., and Danyushevsky, L.V. (1994) Petrology and geochemistry of boninites from the north termination of the Tonga Trench: Constraints on the generation conditions of primary high-Ca boninite magmas. *Journal of Petrology*, 35, 1183–1211.
- Wood, B.J., and Virgo, D. (1989) Upper mantle oxidation state: Ferric iron contents of lherzolite spinels by ^{57}Fe Mössbauer spectroscopy and resultant oxygen fugacities. *Geochimica et Cosmochimica Acta*, 53, 1277–1291.

MANUSCRIPT RECEIVED JULY 23, 1994

MANUSCRIPT ACCEPTED APRIL 29, 1996